High-resolution study of $T_z = +1 \rightarrow 0$ Gamow-Teller transitions in the ^{26}Mg(^{3}He,t)^{26}Al reaction

Kalayar Win,[1,*] Y. Fujita,[2,3,†] Yee Yee Oo,[1,‡] H. Fujita,[2] Y. F. Niu,[4,5] T. Adachi,[2] G. P. A. Berg,[6] G. Colò,[4,7] H. Dohmann,[8] M. Dozono,[9,§] D. Frekers,[8] E.-W. Grewe,[8] K. Hatanaka,[2] D. Ishikawa,[2] R. Kehl,[10] N. T. Khai,[11] Y. Kalmykov,[12] H. Matsubara,[2,‖] P. von Neumann-Cosel,[12] T. Niizeki,[13] T. Ruhe,[8] Y. Shimbara,[2,¶] K. Suda,[2] A. Tamii,[2] J. Thies,[8,**] and H. P. Yoshida[14,††]

[1]*Department of Physics, Yadanabon University, Amarapura, Mandalay Division, Myanmar*
[2]*Research Center for Nuclear Physics, Osaka University, Ibaraki, Osaka 567-0047, Japan*
[3]*Department of Physics, Osaka University, Toyonaka, Osaka 560-0043, Japan*
[4]*Dipartimento di Fisica, Università degli Studi di Milano, via Celoria 16, 20133 Milano, Italy*
[5]*ELI-NP, "Horia Hulubei" National Institute for Physics and Nuclear Engineering, 30 Reactorului Street, RO-077125, Bucharest-Magurele, Romania*
[6]*Department of Physics and the Joint Institute for Nuclear Astrophysics, University of Notre Dame, Notre Dame, Indiana 46556, USA*
[7]*INFN, Sezione di Milano, Via Celoria 16, 20133 Milano, Italy*
[8]*Institut für Kernphysik, Westfälische Wilhelms-Universität, D-48149 Münster, Germany*
[9]*Department of Physics, Kyushu University, Higashi, Fukuoka 812-8581, Japan*
[10]*Institut für Kernphysik, Universität zu Köln, 50937 Köln, Germany*
[11]*Institute for Nuclear Science and Technology, 179 Hoang Quoc Viet, Hanoi, Vietnam*
[12]*Institut für Kernphysik, Technische Universität Darmstadt, D-64289 Darmstadt, Germany*
[13]*Department of Environmental Science and Education, Tokyo Kasei University, Kaga, Itabashi, Tokyo 173-0003, Japan*
[14]*CYRIC, Tohoku University, Aramaki, Aoba, Sendai 980-8578, Japan*

(Received 9 October 2017; published 7 December 2017)

In order to study the $T_z = +1 \rightarrow 0$ Gamow-Teller (GT) transitions in the mass $A = 26$ system, a charge-exchange reaction ^{26}Mg(^{3}He,t)^{26}Al was performed at an incident energy of 140 MeV/nucleon and scattering angle at and near 0°, where T_z is the z component of isospin T defined by $(N - Z)/2$. In this (p,n)-type reaction, it is expected that GT states with $T = 0$, 1, and 2 are excited. An energy resolution of $\Delta E = 23$ keV allowed us to study many discrete states. Most of the prominent states showed 0°-peaked angular distributions, which suggested that they are the states excited by $\Delta L = 0$ GT transitions. Candidates of GT states were studied up to an excitation energy $E_x = 18.5$ MeV. The reduced GT transition strengths, B(GT), were derived assuming the proportionality between cross sections and B(GT) values. Standard B(GT) values were obtained form the ^{26}Si β decay, where the mirror symmetry of $T_z = \pm 1 \rightarrow 0$ GT transitions was assumed. The GT strength, as a whole, is divided in two energy regions: the region of up to 8.5 MeV and the higher-energy region of 8.5–12.8 MeV, where the strength in the latter region distributed like a resonance. The obtained GT strength distribution is compared with the results of random phase approximation calculations. The $T = 2$ GT states are expected in the region $E_x \geqslant 13.5$ MeV. By comparing with the results of (n,p)-type ^{26}Mg(d,^{2}He)^{26}Na and ^{26}Mg(t,^{3}He)^{26}Na reactions, the isospin symmetry of $T = 2$ GT states is discussed. Owing to the high-energy resolution, we could study the decay widths Γ for the states in the $E_x > 9$ MeV region. The $T = 2$ state at 13.592 MeV is not noticeably wider than the experimental energy resolution. The narrow width of the state is explained in terms of isospin selection rules.

DOI: 10.1103/PhysRevC.96.064309

I. INTRODUCTION

Gamow-Teller (GT) transitions are mediated by the spin-isospin ($\sigma\tau$) interaction. They are characterized by an angular momentum transfer $\Delta L = \mathbf{0}$ and spin-isospin flip ($\Delta S = \mathbf{1}$ and $\Delta T = \mathbf{1}$). Owing to this simple character, GT transitions are important tools for the study of nuclear structure [1–5]. In addition, they dominate nuclear weak-interaction processes in the nucleosynthesis [6]. Studies of β decay give the most direct information on the reduced GT transition strength B(GT); an absolute B(GT) value can be derived. However, the excitation energy (E_x) accessible in a β decay is limited by the decay Q value. In addition, there is a rapid decrease in feeding as E_x increases owing to the decrease in the phase-space factor [3,5]. In contrast, in charge-exchange (CE) reactions such as the (p,n), (^{3}He,t), (n,p), (d,^{2}He), and (t,^{3}He), one can observe GT transitions to states at higher excitation energies without the Q-value limitation [4,5].

*Present address: Department of Physics, Pakokku University, Pakokku, Myanmar.
†fujita@rcnp.osaka-u.ac.jp
‡Present address: Department of Physics, University of Mandalay, Mandalay, Myanmar.
§Present address: Center for Nuclear Study, University of Tokyo, Saitama 351-0198, Japan.
‖Present address: Tokyo Women's Medical University, Kawada 8-1, Shinjuku, Tokyo 162-8666, Japan.
¶Present address: CYRIC, Tohoku University, Aramaki, Aoba, Sendai 980-8578, Japan.
**Present address: FH Bielefeld - University of Applied Sciences, 32427 Minden, Germany.
††Present address: Research Center for Nuclear Physics, Osaka University, Ibaraki, Osaka 567-0047, Japan.

In CE reactions, states excited by GT transitions (GT states) become prominent at intermediate incident energies (above 100 MeV/nucleon) and forward angles around 0°. This is because of the $\Delta L = 0$ nature of the GT transitions and the dominance of the $\sigma\tau$ part of the effective nuclear interaction at small momentum transfer q [7,8].

Under these experimental conditions it was found that there is a close proportionality between the GT cross sections and the B(GT) values [7,8],

$$\sigma^{\mathrm{GT}}(q,\omega) \simeq K(\omega)N_{\sigma\tau}|J_{\sigma\tau}(q)|^2 B(\mathrm{GT}) \quad (1)$$

$$= \hat{\sigma}^{\mathrm{GT}} F(q,\omega) B(\mathrm{GT}), \quad (2)$$

where $J_{\sigma\tau}(q)$ is the volume integral of the effective interaction $V_{\sigma\tau}$ at momentum transfer q ($\approx$0), $K(\omega)$ is the kinematic factor, ω is the total energy transfer, and $N_{\sigma\tau}$ is a distortion factor. The value $\hat{\sigma}^{\mathrm{GT}}$ is the unit cross section for the GT transition at $q = \omega = 0$ and a given incoming energy for a system with mass number A. The $F(q,\omega)$ value gives the dependence of the GT cross sections on the momentum and energy transfers. It takes a value of unity at $q = \omega = 0$ and usually decreases gradually as a function of E_x, and can be obtained from distorted-wave Born approximation (DWBA) calculations.

We report on the study of GT transitions from the $T_z = +1$ nucleus ^{26}Mg leading to GT states up to $E_x = 18.4$ MeV in the $T_z = 0$ nucleus ^{26}Al using a (p,n)-type (^{3}He,t) reaction at 140 MeV/nucleon, where T_z is the z component of isospin T defined by $(N - Z)/2$ (see Fig. 1). The ^{26}Mg $\rightarrow$ ^{26}Al GT excitation was first studied at an intermediate incident energy of $E_p = 135$ MeV in a pioneering (p,n) reaction in the 1980s [9]. Their energy resolution (ΔE) was about 350 keV [full width at half maximum (FWHM)]. The advantage of using (^{3}He,t) reactions is its better resolution. In 2003, $\Delta E \approx$ 50 keV (FWHM) was realized in the ^{26}Mg(^{3}He,t)^{26}Al reaction at 140 MeV/nucleon [10] by applying dispersion matching techniques in the beam transportation (see Sec. II). Although,

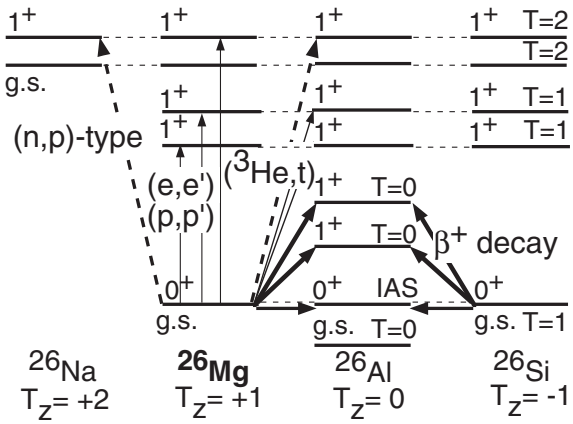

FIG. 1. Schematic view of the isospin analogous states (analog states) and analogous GT transitions in the $A = 26$, $T_z = +2$, $+1$, 0, and -1 isobars, where only ^{26}Mg is stable. The Coulomb displacement energies are removed so that the isospin symmetry of the states and transitions becomes clearer. The type of the reaction or decay is shown alongside the arrow indicating the transition.

in general, a good correspondence of states was observed up to $E_x = 9$ MeV in both reactions, it was found that many states observed in the (p,n) reaction were multiplets even in this lower-energy region.

In 2006, using the same (^{3}He,t) reaction, Zegers *et al.* extended the analysis up to $E_x \approx 20$ MeV region in order to get the whole view of the GT response [11]. In the region above 9 MeV, they observed about 15 states excited with $\Delta L = 0$ transitions. However, since an achromatic beam transportation was used in the (^{3}He,t) reaction [achromatically tuned (^{3}He,t) reaction], the energy resolution was not better than 100 keV, i.e., the energy spread of the ^{3}He beam itself.

In order to obtain detailed structural information on ^{26}Al, we revisit here the ^{26}Mg $\rightarrow$ ^{26}Al GT excitations. By improving the dispersion matching techniques (Sec. II), we could realize a higher-energy resolution of $\Delta E = 23$ keV (FWHM) in the ^{26}Mg(^{3}He,t) reaction. Excitations of many GT states could be studied. In particular, in the $E_x = 8.5$–12.8 MeV region, we could observe a concentration of fragmented GT states. The strengths of them are distributed like a resonance structure. Note that this is the region where Gamow-Teller resonances (GTRs) are expected [4,5,12].

The higher-energy resolution also allows to derive decay widths of states in the GTR region. We found that many states in the $E_x > 9$ MeV region are noticeably broader than the experimental energy resolution. Note that the proton separation energy S_p in ^{26}Al is 6.31 MeV and these states can make proton decay.

Figure 1 shows the isospin analogous structure and the isospin analogous GT transitions in the $A = 26$ isobars. As can be seen, $T_z \pm 1 \rightarrow 0$ GT transitions studied in the ^{26}Mg(^{3}He,t)^{26}Al reaction and the ^{26}Si β decay to ^{26}Al are analogous under the assumption of isospin symmetry (see, e.g., Refs. [5,13,14]) and thus, we can assume that these transitions have the same B(GT) values. Since absolute B(GT) values can be obtained from ^{26}Si β decay, we use the β-decay B(GT) values up to 2.74 MeV [15] for the derivation of the unit GT cross section $\hat{\sigma}^{\mathrm{GT}}$. The B(GT) values for the transitions to higher excited states can be derived using the close proportionality given in Eq. (2).

As illustrated in Fig. 1, the (^{3}He,t) reaction can excite $T = 0$, 1, and 2, $J^\pi = 1^+$ GT states in the $T_z = 0$ nucleus ^{26}Al starting from the $T = 1$, $J^\pi = 0^+$ ground state (g.s.) of the $T_z = +1$ nucleus ^{26}Mg, where $T = 2$ states are situated in the high-energy region. On the other hand, (n,p)-type CE reactions, such as the $(t,^3\mathrm{He})$ reaction or the $(d,^2\mathrm{He})$ reaction can excite only the $T = 2$ analogous GT states situated in the low-energy region of the $T_z = +2$ nucleus ^{26}Na. In Ref. [11], it was suggested that four states in the $E_x = 13.5$–18.5 MeV region of ^{26}Al can be the $T = 2$ GT states by comparing with the results from ^{26}Mg$(t,^3\mathrm{He})$ reaction performed at NSCL, MSU. We could also observe these candidates in the $E_x > 13.5$ MeV region. We compare the B(GT) values for the transitions to these GT states with those derived from ^{26}Mg$(d,^2\mathrm{He})$ [16] and ^{26}Mg$(t,^3\mathrm{He})$ [11] reactions on ^{26}Mg. The narrow peak width of a $T = 2$, 13.592 MeV GT state, situated more than 7 MeV higher than S_p, is discussed in terms of the isospin selection rule.

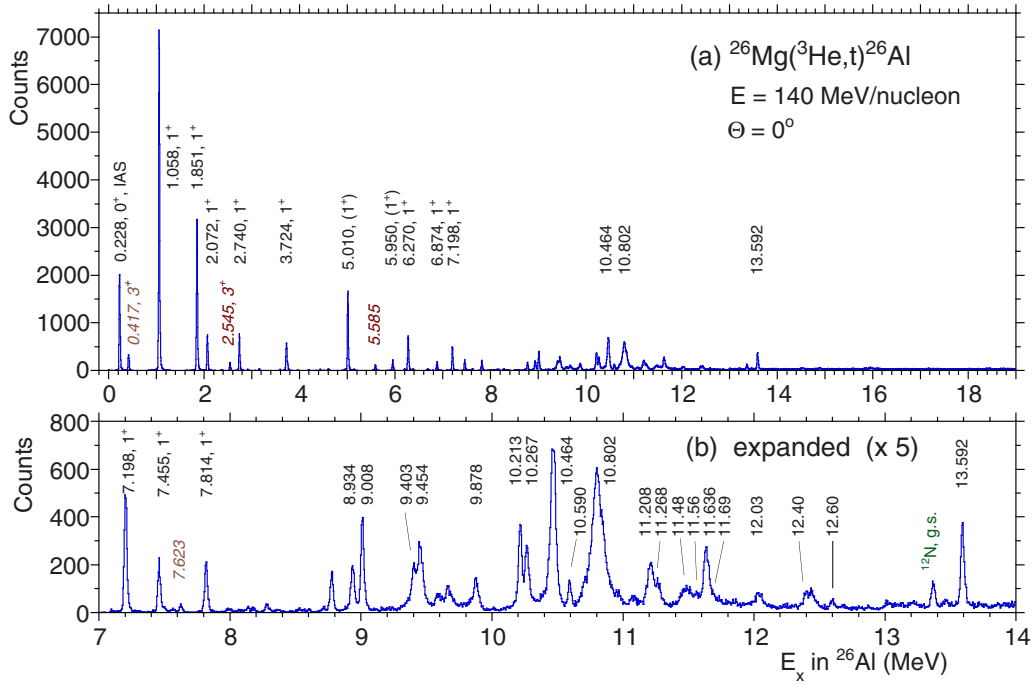

FIG. 2. The ^{26}Mg(^{3}He,t)^{26}Al energy spectrum on two scales, measured at 0° and at an incoming energy of 140 MeV/nucleon. Events with scattering angles $\Theta \leqslant 0.5°$ are included. Most of the prominent states are populated by $\Delta L = 0$ transitions (see Table I and Table II), and we identify that they are GT states, except the isobaric analog state (IAS) at 0.228 MeV. States excited with $\Delta L = 0$ are indicated by their E_x values, where the values up to 8 MeV are taken from Ref. [15]. The states excited with $\Delta L \geqslant 1$ and discussed in the text are indicated by italic characters. All of them are weakly excited at 0°. (a) The full count and full range spectrum. Prominent peaks are observed mainly in the low-lying region below 5 MeV and also in the 9−12 MeV (GTR) region. (b) The energy spectrum of the $E_x = 7$–14 MeV region. The vertical scale is expanded by a factor of 5. Owing to the good energy resolution, many individual states and decay widths of them are observed.

II. EXPERIMENT

The ^{26}Mg(^{3}He,t)^{26}Al experiment was performed at the high-resolution facility of RCNP [17], consisting of the WS course beam line [18] and the Grand Raiden spectrometer [19] using a 140 MeV/nucleon ^{3}He beam from the $K = 400$ Ring Cyclotron [17]. The measurement was performed by setting the spectrometer at 0°. The ^{3}He beam bombarded a self-supporting ^{26}Mg target having an areal density of 0.87 mg/cm^2 and an isotopic enrichment of 99.4%. The current of ^{3}He^{2+} beam was 20–40 nA. A thin target foil was used, because the difference of the atomic energy losses of ^{3}He^{2+} and the triton in the target causes the energy spread of the outgoing triton. The beam was stopped by a Faraday cup placed inside the first dipole magnet of Grand Raiden and the beam current was measured and integrated.

The outgoing tritons were momentum analyzed within the full acceptance of the spectrometer and were focused at the focal plane. The focal-plane detector system consisting of a multiwire drift chamber and two thin plastic ΔE detectors allowed for particle identification and track reconstruction in the horizontal and vertical directions [20]. The acceptance of the spectrometer was subdivided into five angle cuts using the information of tracks (see Sec. III).

An energy resolution far better than the energy spread of the accelerated ^{3}He beam ($\Delta E = 100$–120 keV) was realized by applying dispersion matching techniques between the spectrometer and the beam line (the dispersive mode of the beam transportation) [21], where the faint beam method was used to diagnose the matching conditions [22]. As a result, $\Delta E = 23$ keV (FWHM) (corresponding to $\Delta E/E = 5 \times 10^{-5}$) was realized. The full energy-range spectrum for the scattering-angle cut of $\Theta \leqslant 0.5°$ (the 0° spectrum) is shown in Fig. 2(a). The expanded spectrum of the $E_x = 7$–14 MeV region is shown in Fig. 2(b). As can be seen, many individual states are observed. In addition, we observe broadening of peaks for the states in the $E_x > 9$ MeV region [see Fig. 2(b)] A detailed spectrum of the $E_x = 13$–19 MeV region is shown in Fig. 5(a).

In order to accurately determine the scattering angle Θ around 0° (0°–2° region), angle measurements in both x direction (θ) and y direction (ϕ) are equally important, where Θ is defined by $\Theta \cong \sqrt{\theta^2 + \phi^2}$. Good θ and ϕ resolutions were achieved by applying the angular dispersion matching technique [21] and the "over-focus mode" in the spectrometer [23], respectively. We estimate that the angular resolution $\Delta\Theta$ is ≈5 mr (FWHM) [22].

The ^{26}Mg target used in the experiment contained a small amount of the ^{24}Mg isotope (≈0.5%). In order to identify the ^{24}Al states in the ^{26}Al spectrum, if existing, we compared our ^{26}Al spectrum with that of the ^{24}Al measured in the ^{24}Mg(^{3}He,t) reaction under the same experimental conditions. In our ^{26}Al spectrum, we did not find ^{24}Al peaks corresponding to the strongly excited 1^+ GT states (1.090 MeV and 2.991 MeV states in ^{24}Al).

III. DATA ANALYSIS

The acceptance of the 0° setting of the spectrometer was subdivided into five angle cuts of $\Theta \leqslant 0.5°$, 0.5°–0.8°, 0.8°–1.2°, 1.2°–1.6°, and 1.6°–2.0° by doing a software analysis. For each spectrum generated by the angle cuts, peak positions, and yields of the observed states were obtained using the peak-fitting program S-FIT [24], in which the shape of the well separated peak at 1.058 MeV was used as a reference. Above the S_p value of 6.31 MeV, a continuum caused by quasi-free-scattering (QFS) reactions can appear. In the spectra, the continuous counts become noticeable above $E_x \approx 8.5$ MeV and gradually increase with excitation energy [see Fig. 2(b)]. Therefore, a smooth empirical background connecting the deepest valleys between peaks was subtracted in the peak-fit analysis. The peak counts in the $\Theta \leqslant 0.5°$ spectrum are given in column 6 of Table I and column 3 of Table II for the $E_x = 0$–8.5 MeV region and 8.5–18.5 MeV region, respectively.

In addition, in the $E_x > 9.4$ MeV region, i.e., the region more than 3 MeV higher than S_p, it was found that many states were broader than the lower-lying states due to the decay width [see Fig. 2(b)]. The decay width of each state was derived assuming a Breit-Wigner shape of the broadening using the program S-FIT. Since our energy resolution is 23 keV, we estimate that the minimum decay width that can be extracted is ≈10 keV. The obtained widths Γ are given in column 5 of Table II for states with good statistics.

A. Excitation energy

The E_x values of $J^\pi = 1^+$ GT states in ^{26}Al have been evaluated within uncertainties of 1 keV up to 7.880 MeV state in Ref. [15] (the first column of Table I). The E_x values of higher excited states were determined with the help of kinematic calculations from their peak positions in the $\Theta \leqslant 0.5°$ spectrum. In order to obtain the relationship between the peak positions in the spectrum and the corresponding values of magnetic rigidity of the spectrometer, we took a calibration spectrum for a natural magnesium (^{nat}Mg) target. The ^{nat}Mg target foil was thin (≈1.5 mg/cm^2) and the spectrum was taken under the same experimental conditions as for the ^{26}Mg target. The reaction Q values for the isotopes ^{26}Mg and ^{24}Mg are different by about 10 MeV in the (^{3}He,t) measurements (about −4.0 and −13.9 MeV, respectively). The E_x values of a few low-lying states in ^{24}Al up to 1.090 MeV are known with an accuracy better than 1 keV. In addition, the E_x values of higher excited states in ^{24}Al up to $E_x \approx 6.5$ MeV were determined in a β^+-decay study of ^{24}Si [25], although the uncertainties were larger (≈12 keV). Therefore, all E_x values of ^{26}Al states up to $E_x \approx 16.5$ MeV (Table I and Table II) could be determined by interpolation.

We estimate that the uncertainties of the obtained E_x values are 1–2 keV up to $E_x \approx 9$ MeV for the states having more than ≈500 counts. As can be seen in Table I, we are in good agreement up to $E_x = 7.8$ MeV with the values given in Ref. [15], where precise E_x values with an accuracy better than 1 keV are provided. The derived E_x values are also in good agreement up to 9 MeV with those listed in Ref. [10].

Most of the states in the region between 9–14 MeV have decay widths. Therefore, we estimate uncertainties of ⩽8 keV for the well isolated peaks with good statistics. At 13.36 MeV in the $\Theta \leqslant 0.5°$ ^{26}Al spectrum [0° spectrum, see Fig. 2(b)], we could identify a slightly thick peak corresponding to the g.s. of ^{12}N from the ^{12}C contaminant. Its E_x value (i.e., 0.0 MeV) was reproduced with a deviation of ≈5 keV. It is estimated that the thin ^{26}Mg target was heated homogeneously by the beam irradiation and the ^{12}C contaminant was accumulated on both faces of the target.

For the states in the region between 14 and 16.5 MeV [see Fig. 5(a)], we estimate larger uncertainties of 10–20 keV. In this region, the peak widths are larger and the statistics lower, and thus the peak-decomposition analysis has a larger uncertainty. Since the E_x value of the highest observed state, i.e., 18.5 MeV, was determined by extrapolation, we estimate an uncertainty of ≈30 keV. Above this energy, no sharp peak was observed.

The E_x values of states determined in the achromatically tuned (^{3}He,t) reaction [11] are given in columns 8 and 6 of Tables I and II, respectively. The present E_x values are in agreement within 10 keV with the values in Ref. [11] up to 8 MeV (see Table I). In the GTR region ($E_x \approx 8.5$–12.5 MeV), however, we found that some of the states in Ref. [11] are doublets. In addition, we found a few additional candidates for GT states (see Table II). Possible correspondence of states is discussed in Sec. IV A. Above 13.5 MeV most of the E_x values in Ref. [11] are lower than our values.

B. Assignment of angular momentum transfer ΔL

Due to the $\Delta L = 0$ nature of the GT excitation, it is expected that a GT state has the largest intensity at 0° and smaller intensities at larger angles. On the other hand, states with $\Delta L \geqslant 1$ have larger intensities at larger angles (see Ref. [26] for the angular distributions of states excited with different ΔL). In order to identify the candidates for GT states having such $\Delta L = 0$ nature, relative peak intensities of each state in the five spectra for the different angle cuts mentioned above were examined, where the reference was taken from the prominent 1.058 MeV state, the most strongly excited $J^\pi = 1^+$ GT state.

Many states well excited in the $\Theta \leqslant 0.5°$ spectrum showed relative peak intensities similar to those of the reference peak, suggesting that they are excited with $\Delta L = 0$. On the other hand, weakly excited states in the $\Theta \leqslant 0.5°$ spectrum mostly showed larger peak intensities in larger angle spectra. A state having relative peak intensities within ≈20% compared to those of the reference peak in the five angle cuts was accepted as a $\Delta L = 0$ excitation (for details, see, e.g., Refs. [26,27]). For the weakly excited states and also for the states in the higher E_x region, the $\Delta L = 0$ assignments were less clear. They are indicated by the label "(0)" in Table II.

The result of the ΔL assignment is shown in column 5 and 2 of Table I and II, respectively. Note that most of the prominent states in Figs. 2(a) and 2(b) are assigned as $\Delta L = 0$. It is note that the (^{3}He,t) reaction at 140 MeV/nucleon is strongly selective for the $\Delta L = 0$ excitation in the measurement at 0°.

TABLE I. States of ^{26}Al up to 8.5 MeV and GT transition strengths B(GT). Evaluated values from [15] are given in the first three columns. The results from the present dispersive ^{26}Mg(^{3}He,t)^{26}Al measurement at $E = 140$ MeV/nucleon are shown in columns 4–7. Observed counts of states in the angle range $\Theta \leqslant 0.5^\circ$ are given as Counts (0°). The B(GT) values are derived for the states populated in $\Delta L = 0$ transitions. The results from the achromatically tuned ^{26}Mg(^{3}He,t)^{26}Al reaction [11] are shown in columns 8–9.

Evaluated values [15]			(^{3}He,t): present work				(^{3}He,t) [11]	
E_x (MeV)	J^π; T	β-decay B(GT)[a]	E_x (MeV)	ΔL	Counts (0°)	B(GT)	E_x (MeV)	B(GT)
0.0	5^+		0.0	$\geqslant 1$	46 (8)			
0.2283	0^+; 1 (IAS)		0.230	0	10563 (137)			
0.4169	3^+		0.417	$\geqslant 1$	1794 (59)			
1.0577	1^+	1.098 (26)	1.057	0	38041 (264)	1.089 (26)	1.06	1.090 (30)
1.8506	1^+	0.526 (12)	1.850	0	18639 (183)	0.536 (14)	1.85	0.540 (20)
2.0716	1^+	0.088 (05)	2.070	0	4072 (87)	0.117 (04)	2.07	0.114 (08)
2.3652	3^+		2.364	$\geqslant 1$	76 (10)			
2.5454	3^+		2.544	$\geqslant 1$	801 (38)			
2.7400	1^+	0.110 (05)	2.740	0	3959 (85)	0.115 (04)	2.74	0.119 (08)
2.9134	2^+		2.912	$\geqslant 1$	115 (15)			
3.1600	2^+		3.160	$\geqslant 1$	174 (18)			
3.5963	3^+		3.594	$\geqslant 1$	111 (15)			
3.7238	1^+		3.724	0	3392 (208)	0.099 (06)	3.73	0.109 (08)
3.9628	3^+		3.964	$\geqslant 1$	39 (8)			
4.1919	(3^+)		4.194	$\geqslant 1$	63 (9)			
4.4307	2^-		4.430	$\geqslant 1$	125 (14)			
4.5992	$(3)^+$		4.61	$\geqslant 1$	212 (18)			
4.6224	$(2)^-$							
4.9523	(3^+)		4.955	$\geqslant 1$	50 (20)			
5.0102	(1^+)		5.010	0	9132 (128)	0.271 (07)	5.01	0.280 (10)
5.1417	(2^+)		5.144	$\geqslant 1$	65 (25)			
5.5850	(1)		5.588	$\geqslant 1$	618 (35)			
5.6710	1^+		—					
5.9499	(1^+)		5.951	0	1218 (48)	0.036 (02)	5.94	0.041 (05)
6.0280	(1^+); 1		—					
6.1976	$(1,2^+)$		6.200	$\geqslant 1$	140 (18)			
6.2702	1^+		6.269	0	4178 (90)	0.126 (04)	6.27	0.134 (08)
6.3640	(3^+)		6.368	$\geqslant 1$	138 (19)			
6.6805	(2^+)		6.681	$\geqslant 1$	193 (21)			
6.8743	1^+		6.876	0	882 (41)	0.027 (01)	6.87	0.028 (04)
7.0928	(2^+)		7.094	$\geqslant 1$	51 (15)			
7.1984	1^+		7.199	0	2785 (72)	0.085 (03)	7.20	0.089 (06)
7.4553	1^+		7.457	0	1096 (47)	0.034 (02)	7.46	0.036 (04)
7.6227	(1^+)		7.622	$\geqslant 1$	150 (19)			
7.8136	1^+; 0 + 1		7.815	0	1199 (49)	0.037 (02)	7.81	0.037 (04)
7.8796	(1^+); 0 + 1		—					
7.982(2)	$(2)^+$							
8.0006	$(1)^-$		7.99	$\geqslant 1$	146 (24)			
8.0081	$(2)^+$							
8.130(2)	$(1^-,2^-)$		8.135	$\geqslant 1$	175 (25)			
8.164(2)	(1^-)							
8.174(2)	(3^+)		8.17	$\geqslant 1$	125 (22)			
8.272 (2)	(2^-)		8.280	$\geqslant 1$	200 (22)			

[a]Derived from the ^{26}Si $\rightarrow$ ^{26}Al β-decay data given in Ref. [15].

The 0.229 MeV peak assignedd as the isobaric analog state (IAS) of the g.s. of ^{26}Mg [15] also shows a $\Delta L = 0$ character. It is expected that the Fermi strength is concentrated in the single transition to this IAS. Accordingly, we assume that all states populated in $\Delta L = 0$ transitions, except the IAS, are GT states [5].

In Ref. [15], it is evaluated that the 5.5850 MeV, 5.6710, 6.0280, 7.6227, and 7.8796 MeV states have J^π values of (1), 1^+, (1^+), (1^+), and (1^+), respectively. In the present angular distribution analysis, however, none of them showed the typical $\Delta L = 0$ nature. Our 5.588 MeV state has a relative intensity by ≈30% larger than that of the reference 1^+ state

TABLE II. States of ^{26}Al in the $E_x = 8.5$–18.5 MeV region and GT transition strengths B(GT). The results from the present and achromatically tuned (Ref. [11]) ^{26}Mg(^{3}He,t)^{26}Al reactions are compared. The correspondence of states with those evaluated in Ref. [15] is not clear in this energy region. Observed counts of states in the angle range $\Theta \leqslant 0.5^\circ$ are given in column 3 as Counts (0°). The B(GT) values are derived for the states populated in $\Delta L = 0$ transitions (column 4). Decay widths Γs could be studied for the states with $E_x > 9.4$ MeV with the present experimental resolution of 23 keV. The Γ values are given in column 5 for the states with good statistics. The peak width of the $T = 2$, 13.592 MeV state is not noticeably broader than the experimental energy resolution (see the discussion in Sec. IV D).

(^{3}He,t) present work					(^{3}He,t) [11]	
E_x (MeV)	ΔL	Counts (0°)	B(GT)	Γ (keV)	E_x (MeV)	B(GT)
8.780	$\geqslant$1	967 (46)				
8.934	0	1698 (60)	0.053 (02)			
					8.98	0.123 (08)
9.008	0	2355 (71)	0.074 (03)			
9.38	$\geqslant$1	–				
9.403	0	2517 (109)	0.079 (04)	31 (6)		
					9.43	0.136 (08)
9.454	0	3109 (113)	0.098 (04)	28 (6)		
9.59	$\geqslant$1	623 (84)				
					9.62	0.079 (07)
9.663	$\geqslant$1	1339 (70)				
9.878	0	1747 (71)	0.056 (03)	38 (5)	9.86	0.058 (06)
10.213	0	3090 (94)	0.099 (04)	13 (2)		
					10.24	0.158 (09)
10.267	0	2265 (89)	0.073 (03)	18 (2)		
10.464	0	8494 (138)	0.273 (08)	25(5)	10.45	0.290 (10)
10.590	0	878 (109)	0.028 (03)			
10.802	0	14840 (190)	0.480 (13)	69 (8)	10.81	0.470 (20)
10.96	$\geqslant$1	258 (42)				
11.08	$\geqslant$1	621 (55)				
11.208	0	2537 (94)	0.083 (04)	40 (7)		
					11.22	0.164 (09)
11.268	0	1270 (79)	0.041 (03)	23 (5)		
11.48[a]	0	1620 (180)	0.053 (06)	(48)	11.50	0.021 (05)
11.56 [a]	(0)	569 (140)	0.019 (04)			
11.636[a]	0	3365 (105)	0.111 (04)	24 (6)	11.62	0.170 (10)
11.69	(0)	547 (73)	0.018 (02)			
12.03	(0)	577 (128)	0.019 (04)		12.01	0.015 (03)
12.40	(0)	699 (72)	0.023 (02)		12.41	0.022 (04)
12.43	$\geqslant$1	858 (78)				
12.60	(0)	332 (39)	0.011 (01)			
13.592	0	1996 (92)	0.068 (04)	<10	13.57	0.068 (03)
14.54	(0)	528 (54)	0.018 (02)		14.53	0.015 (04)
14.90	(0)	400 (46)	0.014 (02)		14.88	0.018 (05)
15.96	(0)	609 (73)	0.022 (03)		15.91	0.029 (06)
18.43	(0)	543 (62)	0.020 (02)		18.32	0.021 (05)

[a]States at 11.48 MeV, 11.56 MeV, and 11.636 MeV form a triplet and all have decay widths. The decay width for the 11.48 MeV state is less certain. The decay width for the 11.56 MeV state was difficult to obtain.

(i.e., 1.057 MeV, 1^+ state) in the highest angle-cut spectrum of 1.6°–2.0°. It is found that its angular distribution is rather similar to the 0.4169 MeV and the 2.5454 MeV, 3^+ states. The 7.622 MeV state, which is weakly excited in the 0° spectrum, shows a rapidly increasing angular distribution characteristic of $\Delta L \geqslant 1$ states. Other states expected at 5.6710 MeV, 6.0280 MeV, and 7.8796 MeV were not observed.

In comparison with the achromatically tuned (^{3}He,t) reaction [11], it was found that both experiments are in agreement for the assignments of $\Delta L = 0$ states up to $E_x = 8$ MeV (see Table I). However, in the higher-E_x region, we see that some of their states are doublets (see the discussion in Sec. IV A and Table II).

Owing to the good energy resolution, many weakly excited states (counts ≈50–300 in the $\Theta \leqslant 0.5^\circ$ spectrum) could be observed in the lower-E_x region of <8.5 MeV. It was found that all of them have typical $\Delta L \geqslant 1$ angular distributions that increase at larger angles. For most of these weakly excited states, candidates for corresponding states can be found in Ref. [15]. Their excitation energies are given in the first column of Table I. In the $E_x > 8.5$ MeV region, however, identification of weakly excited $\Delta L \geqslant 1$ states was difficult because of the

higher level density and also the quasifree continuum that gradually increases above S_p.

C. Evaluation of B(GT) values

Counts of individual states in the $\Theta \leqslant 0.5^\circ$ angle cut obtained in the peak-decomposition analysis are shown as "Counts (0°)" in Tables I–II. The reduced GT transition strength B(GT) is derived for each $\Delta L = 0$ state using this value and the close proportionality given by Eq. (2). In order to use this relationship, we need reference B(GT) value(s) and have to derive the unit counts for the unit B(GT). First, we rely on isospin symmetry in isobars. As can be seen in Fig. 1, GT transitions in the $T_z = -1 \rightarrow 0$ β decay from the 0^+ g.s. of ^{26}Si and the $T_z = +1 \rightarrow 0$ ^{26}Mg(^{3}He,t) reaction reaching to the same low-energy 1^+ states in ^{26}Al are analogous (mirror GT transitions). We assume that B(GT) values are equal for a pair of analogous GT transitions.

In β decay, the reduced GT strength B_j(GT) for the GT transition to the jth state is expressed using the ft value as

$$B_j(\mathrm{GT})\lambda^2 = K/f_j t_j, \tag{3}$$

where $K = 6143.6(17)$ [28], $\lambda = g_A/g_V = -1.270(3)$ [29], f_j is the β-decay phase-space factor calculated using the decay Q value, and t_j is the partial half-life. Using the logft values obtained in the ^{26}Si β decay [15], the B(GT) values could be derived for the four GT transitions to low-lying states in ^{26}Al applying Eq. (3). The calculated values are listed in column 3 of Table I.

The B(GT) values of other GT states were calculated using the close proportionality given in Eq. (2). In order to evaluate the E_x dependence of $F(q,\omega)$, a DWBA calculation was performed for the ^{26}Mg(^{3}He,t)^{26}Al reaction using the computer code DW81 [30] following the procedure described in Refs. [31–33]. The optical potential parameters were taken from Ref. [34] (for details, see Ref. [26]).

In order to obtain the unit cross section (or unit count) of B(GT), we selected two largest β-decay B(GT) values of 1.098(26) and 0.526(12) for the transitions to the 1.058 MeV and 1.851 MeV states, respectively (see column 3 of Table I). By using this unit cross-section, a good agreement has been achieved for the corresponding B(GT) values in the β decay and the present (^{3}He,t) reaction (column 3 and 7 of Table I, respectively), which suggests that the close proportionality in Ref. [7] works for these GT transitions to the low-lying states.

In the (^{3}He,t) reaction performed at an intermediate energy of 140 MeV/nucleon, states excited with $\Delta L = 0$ transitions are most probably GT states [5]. Therefore, B(GT) values are calculated for all $\Delta L = 0$ states. The obtained B(GT) values are given in column 7 of Table I and column 4 of Table II.

IV. DISCUSSION

A. Gamow-Teller strength distribution in ^{26}Al

Owing to the high-energy resolution, many individual states were observed even in the GTR region of $E_x = 8.5$–12.5 MeV. Such a fine structure of the GTR is reported in the heavier sd-shell nucleus ^{37}Ar ($T_z = +1/2$) in the ^{37}Cl(^{3}He,t)^{37}Ar reaction [27]. Fine structures are also reported in pf-shell nuclei ^{50}Mn, ^{54}Co, and ^{58}Cu ($T_z = 0$) [35–38], ^{47}V ($T_z = +1/2$) [39], ^{48}V and ^{60}Cu ($T_z = +1$) [5,40], ^{62}Cu ($T_z = +2$) [5], and ^{64}Cu ($T_z = +3$) [5,41]. However, the GTR structure was not found in ^{42}Sc ($T_z = 0$) [26] and was not clear in ^{46}V ($T_z = 0$) [38,42] as well as ^{44}Sc ($T_z = +1$) [43]. Note that the observed features of the strength distributions and the fragmented GTR structures are distinctively different in these sd- and pf-shell nuclei, showing a marked individuality of their structures (see the discussion in Refs. [26,38]).

1. *Fine structure of states in the Gamow-Teller resonance region*

In Tables I and II, results from the present work are compared with those from the achromatically tuned (^{3}He,t) reaction [11]. As mentioned, good agreements are seen up to $E_x = 8$ MeV, while some differences are observed in the GTR region of $E_x \approx 8.5$–12.5 MeV, where the level density is higher. We see in Table II that the state observed at 8.98 MeV in Ref. [11] is now resolved into two states at 8.934 and 9.008 MeV [see also Fig. 2(a)]. We found that both of them are excited with $\Delta L = 0$ and the sum of their B(GT) values is comparable to that of the 8.98 MeV state in Ref. [11].

In a similar way, the 9.43 MeV state is now resolved into the 9.403 MeV and 9.454 MeV states, the 10.24 MeV state into the 10.213 MeV and 10.267 MeV states, and the 11.22 MeV state into the 11.208 MeV and 11.268 MeV states, where the sums of our B(GT) values all correspond to the B(GT) values given in Ref. [11] within their error bars. In the $E_x = 11.4$–11.7 MeV region, we observed four states. In Ref. [11] only two states were recognized at 11.50 and 11.62 MeV. However, the total B(GT) strength is again about the same. Therefore, we see that their total B(GT) strength is redistributed into the four states at 11.48, 11.56, 11.636, and 11.69 MeV.

2. *Overview of the Gamow-Teller strength distribution*

The obtained GT strength distribution is shown in Fig. 3(a), and the cumulative sum in Fig. 3(b). We see that the GT strength concentrates in two energy regions. About 58% of the observed strength is in the region below $E_x \approx 8.5$ MeV and about 38% of the strength is in the energy region of 8.5–12.5 MeV, i.e., the GTR region. Above this region, one sharp state at 13.592 MeV and four weakly excited states were identified as GT states.

In a simple shell-model (SM) picture, we expect two kinds of GT excitations caused by neutron $d_{5/2}$ to proton $d_{5/2}$ transition ($\nu d_{5/2} \rightarrow \pi d_{5/2}$) in the low-energy region and the $\nu d_{5/2} \rightarrow \pi d_{3/2}$ transition in the higher-energy region. The latter excitation is expected to be higher by ≈5–6 MeV than the former owing to the spin-orbit ($L \cdot S$) splitting [1]. The single-particle transition strengths of these GT excitations are similar, namely $B(\mathrm{GT}) = 7/5$ and $8/5$, respectively [7]. Taking the occupation and vacancy factors of the $d_{5/2}$ and $d_{3/2}$ shells of ^{26}Mg into account, the relative strength between the $\nu d_{5/2} \rightarrow \pi d_{5/2}$ and $\nu d_{5/2} \rightarrow \pi d_{3/2}$ transitions is 7 : 24. Therefore, we cannot explain the stronger B(GT) strength in the low-energy region in the simple SM picture without taking effects of the residual interactions into consideration.

It has been widely discussed that the residual pairing interaction with the repulsive nature is active in particle-hole

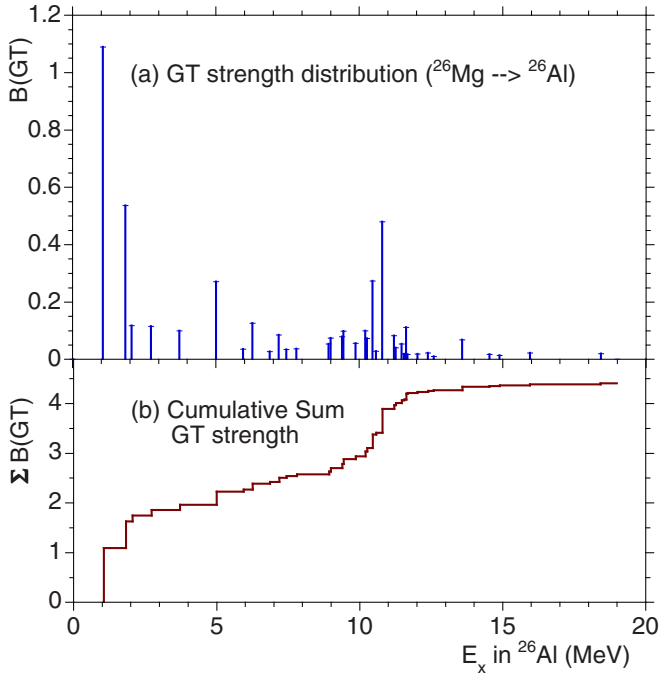

FIG. 3. (a) The B(GT) strength distribution as a function of excitation energy (E_x) in the final nucleus ^{26}Al. Compared to the peak height of the energy spectrum shown in Fig. 2(a), the strengths in the GT resonance (GTR) region of 8–12.5 MeV appears to be larger. This is due to the broad peak widths of the states in this region. (b) Cumulative-sum strength of the experimental B(GT) values. The GT strength is divided into the low-lying ($E_x < 7$ MeV) region and the GTR.

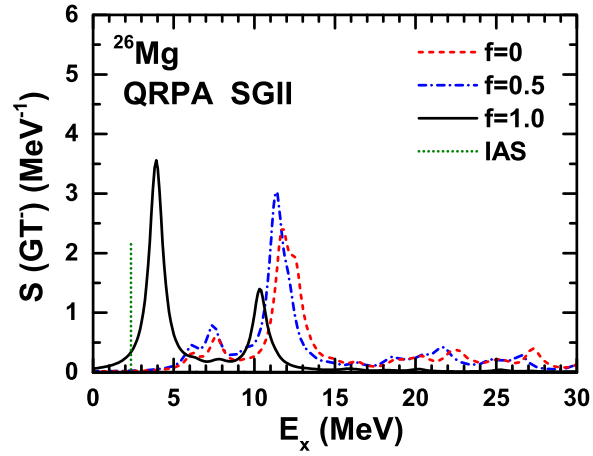

FIG. 4. Strength distributions of the ^{26}Mg $\rightarrow$ ^{26}Al GT transitions obtained by HFB + spherical-QRPA calculations using the Skyrme interaction SGII. The vertical dotted line (seen at 2.3 MeV) is the calculated IAS position (seen at 0.23 MeV in the experiment). The IS pairing interaction can be included in the QRPA calculation. As the IS strength ratio f increases, the GT strength moves to lower E_x. In addition, the lower-E_x peak accumulates more GT strength.

(p-h) configurations in GT excitations (see, e.g., Ref. [44]). Owing to the repulsive nature, it is expected that the GT strength is mainly pushed up to the higher-E_x region and forms the GTR structure (see, e.g., Refs. [5,12,38,45]). On the other hand, in open-shell nuclei, the isoscalar (IS)-type residual pairing interaction is active in proton-particle–neutron-particle (πp-νp) configurations in GT excitations. Owing to the attractive nature of the IS interaction, it is expected that the GT strength is pulled down to the lower-E_x region [26,38,44,45]. In fact, in the measurement of GT transitions from ^{42}Ca to ^{42}Sc having mainly πp-νp configurations [i.e., the $\pi f_{7/2}$-$\nu f_{7/2}$ and $\pi f_{5/2}$-$\nu f_{7/2}$ configurations] on the ^{40}Ca core, it has been observed that the GT strength mostly concentrates in the lowest 1^+ GT state at 0.611 MeV in ^{42}Sc [which is called the low-energy super Gamow-Teller state (LeSGT state)] and only a little GT strength remains in the GTR region [26,38].

Here, we try to understand the overall qualitative feature of the observed GT strength distribution in ^{26}Al from a viewpoint of the interplay between the residual p-h interaction and the IS πp-νp interaction. In order to examine the effects of these interactions, we performed a self-consistent Hartree-Fock Bogoliubov (HFB) plus quasiparticle random phase approximation (QRPA) calculation [45,46] using the Skyrme interaction SGII [47].

First, we performed a standard calculation including the usual isovector (IV), $T = 1$ pairing interaction both in the HFB and QRPA calculation. Then, we introduced the IS πp-νp interaction, i.e., the IS, $T = 0$ pairing interaction, in the QRPA part of the calculation. Its strength is expressed by the proportionality factor f defined by the ratio of the IS pairing interaction strength compared to that of the IV pairing interaction (for details, see Refs. [45,46]). The obtained GT strength distribution as a function of f is shown in Fig. 4, where the E_x values are given with respect to the final nucleus ^{26}Al.

We see that the GT strength is mainly divided into the lower- and higher-energy peaks, which can be qualitatively explained by the involvement of transitions $\nu d_{5/2} \rightarrow \pi d_{5/2}$ and $\nu d_{5/2} \rightarrow \pi d_{3/2}$, respectively. When $f = 0$, i.e., without the IS pairing interaction, the GT strength is mainly concentrated in the higher-energy peak situated in the GTR region of $E_x \approx 12.5$ MeV (dashed line in Fig. 4). In addition, we see fragmented weak GT strength up to high-E_x region.

With the increase of f, the peak positions, in particular the lower-energy peaks, move to lower E_x and at the same time the lowest peak collects more GT strength. Finally, with $f = 1$, i.e., the same IS pairing strength as the IV one, we see that (1) about 2.5 times larger GT strength is in the low-lying region than in the GTR region (solid line in Fig. 4). In addition, (2) the fragmented weak GT strength up to high-E_x region almost disappears. These features are in qualitative agreement with the results seen in our (^{3}He,t) measurement (see Fig. 3). The calculation with $f = 1$ shows that the low-lying state in Fig. 4 is made up mainly with the transition of $\nu d_{5/2} \rightarrow \pi d_{5/2}$ and also $\nu s_{1/2} \rightarrow \pi s_{1/2}$. On the other hand, the GTR is made up mainly with the transition of $\nu d_{5/2} \rightarrow \pi d_{3/2}$ and also $\nu d_{3/2} \rightarrow \pi d_{3/2}$.

Note that the appropriate value of the proportionality factor f is still under discussion, because the strength of the IS pairing interaction has not yet been very firmly constrained. We

find here that the present experimental result is in agreement with the choice of $f \approx 1$ suggested in Ref. [48].

B. Ratio of Gamow-Teller and Fermi transition strengths

Similar to the close proportionality between the GT cross sections and B(GT) values given by Eq. (2), we can expect a close proportionality between the Fermi cross section and the B(F) value in CE reactions at intermediate energies [7],

$$\sigma^{\mathrm{F}}(q,\omega) \simeq \hat{\sigma}^{\mathrm{F}} F(q,\omega) B(\mathrm{F}), \quad (4)$$

where $\hat{\sigma}^{\mathrm{F}}$ is the unit cross section for the Fermi transition at $q = \omega = 0$ and a given incoming energy for a system with mass number A. The value $F(q,\omega)$ gives the dependence of the Fermi cross sections on the momentum and energy transfers. The R^2 value defined as the ratio of the unit GT and Fermi cross sections at $q = \omega = 0$ [7]

$$R^2 = (\hat{\sigma}^{\mathrm{GT}}/\hat{\sigma}^{\mathrm{F}}) = \left[\sigma_i^{\mathrm{GT}}(0)/B_i(\mathrm{GT})\right] / \left[\sigma^{\mathrm{F}}(0)/B(\mathrm{F})\right] \quad (5)$$

is an important value representing the ratio of strengths of the τ and $\sigma\tau$ terms of the effective interaction at a specific beam energy and for a specific mass A.

Assuming that the transition to the IAS at 0.228 MeV has $B(\mathrm{F}) = |N - Z| = 2$, i.e., the total sum rule value, and using the $B(\mathrm{GT}) = 1.089(26)$ of the 1.058 MeV state, a value $R^2 = 6.64(19)$ is derived. This value is in agreement with a value of 6.6(2) deduced in Ref. [10]. It is known that R^2 value smoothly and gradually increases as a function of A in the (^{3}He,t) reaction at 140 MeV/nucleon [49,50]. For example, in a ^{18}O(^{3}He,t)^{18}F measurement, a value of 6.46(6) is derived [51], while in the ^{34}S(^{3}He,t)^{34}Cl measurement, a value of 7.0(5) has been reported [52]. We should, however, mention that a constant value of R^2 independent of mass number A has been suggested in (p,n) reactions at intermediate energies [7].

C. $T = 2$ Gamow-Teller states in ^{26}Al and ^{26}Na

The target nucleus ^{26}Mg has the isospin value $T_i = 1$. Due to the $\Delta T = 0, \pm 1$ nature of the $\sigma\tau$ (GT) operator, $T_f = 0, 1$, and 2 GT states in ^{26}Al are excited in the ^{26}Mg(^{3}He,t) reaction (see Fig. 1). On the other hand, in the (n,p)-type CE reactions, only the $T_f = 2$ GT states are excited in the final nucleus ^{26}Na owing to their $T_z = +2$ nature [5]. Therefore, a pair of states that are commonly observed in the high-E_x region of ^{26}Al and the low-E_x region of ^{26}Na can be isospin analogous states (analog states) with $T = 2$.

1. *Identification of $T = 2$ Gamow-Teller states*

The states in the $E_x > 13.5$ MeV region observed in the achromatically tuned ^{26}Mg(^{3}He,t)^{26}Al measurement were compared with the low-lying states observed in the (n,p)-type ^{26}Mg(t,^{3}He)^{26}Na reaction at $E_t = 115$ MeV/nucleon [11]. It was suggested that the states observed at 13.57 MeV and higher energies (14.88, 15.91, and 18.32 MeV states) in ^{26}Al are candidates for the $T = 2$ states (see column 3 and 5 of Table III). Among them, it was identified that the 13.57 MeV state was the analog state of the $J^\pi = 1^+$, 0.08 MeV state in ^{26}Na.

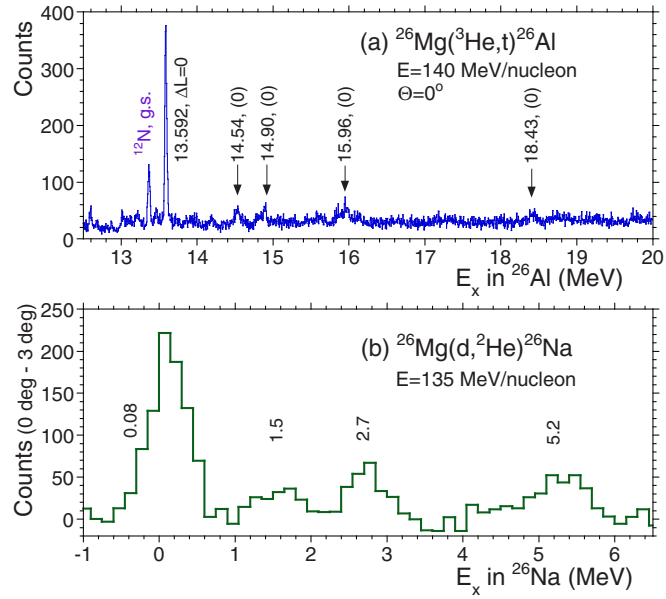

FIG. 5. Comparison of ^{26}Mg(^{3}He,t)^{26}Al and ^{26}Mg(d,^{2}He)^{26}Na spectra. (a) The $E_x = 12.5 - 20$ MeV region of the 0°, ^{26}Mg(^{3}He,t)^{26}Al spectrum. States excited with $\Delta L = 0$ or probably with $\Delta L = 0$ [indicated by (0)] are shown by their E_x values. (b) The ^{26}Mg(d,^{2}He)^{26}Na spectrum at $E_p = 135$ MeV/nucleon [16] up to 6.5 MeV. In order to enhance the forward-peaked states excited with $\Delta L = 0$, the 3° spectrum is subtracted from that of 0°. Corresponding isobaric analog GT states are observed in $T_z = 0$ nucleus ^{26}Al and $T_z = +2$ nucleus ^{26}Na.

We show here a comparison of states observed in the present (^{3}He,t) measurement (the first column of Table III) and the (n,p)-type ^{26}Mg(d,^{2}He)^{26}Na reaction at $E_d = 135$ MeV/nucleon performed at the SMART magnetic spectrometer at RIKEN [53]. The details of the experimental procedure and the results of the analysis of the (d,^{2}He) measurement are given in Ref. [16]. The energy resolution was ≈600 keV (FWHM).

Figure 5(a) shows the $E_x = 12.5$–20 MeV region of the present (^{3}He,t) spectrum at 0°. The (d,^{2}He) spectrum up to $E_x = 6.5$ MeV is shown in Fig. 5(b). In order to enhance the forward-peaked states excited with $\Delta L = 0$, the 3° spectrum is subtracted from that of 0° after correcting the different acceptances of the spectrometer at these two angles. Candidates of GT states are indicated by their E_x values [16] and listed in column 7 of Table III.

Since resolutions of these two spectra are very different, it is not clear if a state corresponding to the 14.54 MeV state in Fig. 5(a) also exists in Fig. 5(b). Note that the analog state, if excited at all, is expected at $E_x \approx 1.03$ MeV in ^{26}Na. In the evaluation given in Ref. [15], however, no corresponding state with $J^\pi = 1^+$ is reported (see the last column of Table III). Therefore, in accordance with Ref. [11], we also suggest that the 14.54 MeV state is not a $T = 2$ state.

2. *Coulomb displacement energies of the $T = 2$ states*

The first and the third columns of Table III show the E_x values of the candidates of GT states observed above 13.5 MeV

TABLE III. Candidates of GT states in the $E_x = 13.5$–18.5 MeV region in ^{26}Al and in the $E_x \leqslant 5.5$ MeV region in ^{26}Na. The results from the present (^{3}He,t) reaction are compared with those obtained in the achromatically tuned (^{3}He,t) reaction [11], a (t,^{3}He) reaction [11], and a (d,^{2}He) reaction [16]. Evaluated E_x values of (possible) 1^+ states in ^{26}Na [15] are listed in the last column.

(^{3}He,t) present work		(^{3}He,t) [11]		(t,^{3}He) [11]		(d,^{2}He) [16]		^{26}Na states[a] [15]
E_x(MeV)	B(GT$^-$)[b]	E_x(MeV)	B(GT$^-$)[b]	E_x(MeV)	B(GT$^+$)	E_x(MeV)	B(GT$^+$)	E_x(MeV)
13.592 [0.08][c]	0.41(2)	13.57	0.41(2)	0.08	0.42(3)	0.08	0.37	0.082(1)
14.54[d] [1.03][c]	0.11(1)	14.53[d]	0.09(2)					
14.90 [1.39][c]	0.08(1)	14.88	0.11(3)	1.4(2)	0.09(2)	1.5	0.07	1.509(1)
15.96 [2.45][c]	0.13(3)	15.91	0.17(4)	2.6(2)	0.13(2)	2.7	0.12	2.720(3)
18.43 [4.92][c]	0.12(2)	18.32	0.13(6)	5.1(4)	0.22(4)	5.2	0.11	

[a]States assigned to be $J^\pi = 1^+$ or (1^+).
[b]Experimentally obtained B(GT) values are multiplied by a factor of 6 in order to compensate the difference of Clebsch-Gordan (CG) coefficients in (p,n)-type and (n,p)-type reactions (see text).
[c]Expected E_x value in ^{26}Na assuming that the 13.592 MeV state corresponds to the 1^+ state at 0.082 MeV.
[d]Corresponding analog state is not found in ^{26}Na (see Ref. [15]).

in the present and achromatically tuned (^{3}He,t) reactions. We know here that the lowest $T = 2$ state at 13.592 MeV is the analog state of the 0.082 MeV, 1^+ state in ^{26}Na. Therefore, the E_x values of the higher excited $T = 2$ analog GT states in ^{26}Na can be estimated under the assumption of the isospin symmetry in the $A = 26$ isobars. The estimated E_x values are given in the square brackets (the first column of Table III).

We see that these estimated E_x values of ^{26}Na states are 100 and 300 keV smaller than those of the evaluated ^{26}Na states at 1.5 and 2.7 MeV, respectively (see the last column of Table III [15]). As mentioned, the E_x values derived in the present (^{3}He,t) measurement are determined with an uncertainty of $\approx$20 keV. Taking this accuracy into account, we can safely say that the Coulomb displacement energies (CDEs) of these high-E_x states, and thus the binding conditions of these states, are largely dependent on their E_x values. It has been discussed that CDE values are also dependent on the relevant configurations [54–56].

3. *Gamow-Teller transition strengths to the $T = 2$ states*

Let us examine the difference of B(GT) values in a pair of isospin analogous GT transitions starting from the $T = 1$ g.s. of ^{26}Mg ($T_z = +1$). First we see that the squared value of isospin Clebsch-Gordan (CG) coefficient for a GT transition to a $T = 2$ GT state in ^{26}Na ($T_z = +2$) is unity (see, e.g., Ref. [5]). On the other hand, the one to the analog GT state in ^{26}Al ($T_z = 0$) is 1/6. Therefore, it is expected that the B(GT) value to a $T = 2$ state obtained in β^+-type ^{26}Mg $\rightarrow$ ^{26}Na reactions [B(GT$^+$) value] is six times larger than the one obtained in β^--type ^{26}Mg $\rightarrow$ ^{26}Al reactions. Thus, in order to make a direct comparison with the B(GT$^+$) values from the β^+-type (t,^{3}He) and (d,^{2}He) reactions, the B(GT) values from the β^--type (^{3}He,t) reactions given in Table II ought to be multiplied by a factor of 6. These modified values [B(GT$^-$) values] are listed in Table III (columns 2 and 4).

Good agreement of B(GT$^-$) and B(GT$^+$) values is seen for GT transitions from the g.s. of ^{26}Mg to the pair of analog states at 13.592 MeV in ^{26}Al and at 0.08 MeV in ^{26}Na. Reasonable agreement is also apparent for the other three pairs of excited states.

D. Decay widths of states

For the states above the proton separation energy $S_p = 6.31$ MeV, proton decay becomes possible. Since the proton decay is a fast process, lifetimes of states can be short, and thus states can have a decay width Γ. The Γ value is small in the region just above S_p owing to the Coulomb barrier, while a larger width is expected at higher E_x regions. We could derive decay widths for the states with $E_x \geqslant 9.40$ MeV, i.e., for the states in the GTR region (see column 5 of Table II). Here, we try to interpret the features of the observed decay widths for the states in the GTR region and also for the 13.6 MeV, $T = 2$ state.

1. *Estimation of the decay width*

In order to estimate how the decay width of a GT state changes as a function of excitation energy, we performed a continuum random phase approximation (RPA) calculation using the interaction SGII [47]. This calculation can take the coupling with the continuum into account and properly deduce the decay widths of states (for details, see Ref. [57]). Since only the p-h residual interaction is included in the calculation, the GT strength is mainly concentrated in a single peak corresponding to the GTR.

When the original SGII interaction is used, the peak appears at $E_x = 8.5$ MeV. This E_x value is $\approx$2 MeV lower than the experimental value of $\approx$10.5 MeV of the GTR and also only 2.2 MeV higher than the S_p value of 6.3 MeV. At this peak position of 8.5 MeV, the predicted decay width is significantly smaller than the experimental detection limit of $\Gamma \approx 10$ keV. By applying a renormalization factor in the calculation of residual-interaction matrix elements, we can shift the GTR peak to higher energies, and then examine the width of the peak at each specific energy. With the renormalization factor of 1.5, the GTR peak moves up to $E_x = 10.3$ MeV and a Γ value of $\approx$10 keV is calculated. When the factor is increased up to 1.7 and 1.8, the peak positions further move up to 10.9 MeV and 11.2 MeV, respectively, and the corresponding decay widths of 50 and 90 keV are calculated. By comparing with the Γ values given in Table II, we see that the experimentally

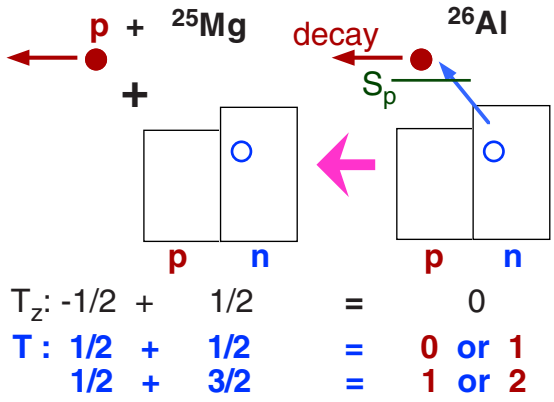

FIG. 6. Isospin selection rules in the proton decay from excited states of ^{26}Al. The z component of isospin T, i.e., T_z follows the (scalar) addition rule. On the other hand, vector nature should be taken into account in the addition of T values. As a result, a $T = 2$ state in ^{26}Al cannot decay into a low-lying $T = 1/2$ states in ^{25}Mg and a proton. It can decay only into a $T = 3/2$ state existing at $E_x = 7.79$ MeV and higher and a proton. For details, see text.

observed decay width at each excitation energy is reasonably well reproduced.

2. *Decay width of the 13.592 MeV, $T = 2$ state*

In the higher-E_x region, an interesting observation is made; the 13.592 MeV, $T = 2$ state is sharp and its peak width is not appreciably broader than the ones of the states in the low-lying region [see Fig. 2(b)]. We find that the narrow peak width of this $T = 2$ state can be explained in terms of isospin selection rules in the proton decay of a ^{26}Al state shown in Fig. 6 schematically.

First, let us think of the proton decay of a $T = 0$ or 1 state in ^{26}Al. As can be seen from the selection rules shown in the lower part of the figure, both $T = 0$ and 1 states can decay into a proton with $T = 1/2$ and a low-lying ^{25}Mg state having $T = 1/2$ and $E_x(T = 1/2)$, if the E_x values of the initial states in ^{26}Al exceed $S_p + E_x(T = 1/2)$, i.e., $6.31 + E_x(T = 1/2)$ MeV.

On the other hand, a $T = 2$ state in ^{26}Al can decay only into a proton and a $T = 3/2$ state in ^{25}Mg, where the lowest $T = 3/2$ state in ^{25}Mg is situated relatively high (at $E_x = 7.79$ MeV). Therefore, the proton decay of $T = 2$ states in ^{26}Al is allowed only for the states located higher than $S_p + E_x(T = 3/2)$, i.e., $6.31 + 7.79 = 14.10$ MeV. Therefore, the 13.592 MeV, $T = 2$ state, in principle, cannot make proton decay and is kept sharp.

In reality, however, isospin T is not a good quantum number and a small amount of impurity is expected (see, e.g., Ref. [58]). Therefore, what we can say is that the proton decay of the 13.592 MeV, $T = 2$ state is suppressed and its decay width Γ is $\leqslant 10$ keV, i.e., the experimental detection limit.

V. SUMMARY

In summary, GT excitations were studied by the ^{26}Mg(^{3}He,t)^{26}Al reaction at 140 MeV/nucleon and at 0°. At an energy resolution of 23 keV, many fragmented states were observed. Many of the prominent states were excited with $\Delta L = 0$ transition. Good correspondence was observed between most of these $\Delta L = 0$ excited states and the known $J^\pi = 1^+$ GT states up to 8 MeV, indicating that the (^{3}He,t) reaction is sensitive to GT excitation. The GT states in ^{26}Al were studied up to 18.5 MeV, where E_x values could be derived by interpolation up to ≈17 MeV.

The GT transition strengths, the B(GT) values, were derived assuming the close proportionality between cross sections and B(GT) values. The reference B(GT) value was obtained from the ^{26}Si β-decay measurements, where the mirror symmetry between $T_z = \pm 1 \rightarrow 0$ GT transitions was assumed. The GT strength was mainly distributed in two energy regions, i.e., the lower-E_x region of <8.5 MeV and the GTR region of $E_x =$ 8.5–12.5 MeV, where about 58% of the observed strength was found in the lower-E_x region. The QRPA calculations showed that the IS-type attractive residual interaction plays an important role to shift the GT strength to the lower-energy region.

Starting from the $T = 1$ g.s. of ^{26}Mg, the (p,n)-type (^{3}He,t) reaction can excite GT states with $T = 0, 1$, and 2 in ^{26}Al. On the other hand, (n,p)-type CE reactions excite only $T = 2$ states in ^{26}Na. Note that the GT transitions from the g.s. of ^{26}Mg to the $T = 2$ states in ^{26}Al and ^{26}Na are analogous. We compared the B(GT) values of the analogous transitions to the $T = 2$ GT states in ^{26}Al and ^{26}Na obtained, respectively, in the present ^{26}Mg(^{3}He,t)^{26}Al reaction and in the (n,p)-type ^{26}Mg(d,^{2}He)^{26}Na reaction. After a proper correction of the geometrical factors (i.e., the CG coefficients), it was found that the B(GT) values in these (p,n)- and (n,p)-type CE reactions were the same within the experimental uncertainties. A similar conclusion was reached in the comparison of the present results with the (n,p)-type ^{26}Mg(t,^{3}He)^{26}Na reaction.

Owing to the high-energy resolution achieved in the ^{26}Mg(^{3}He,t)^{26}Al reaction, we could observe larger peak widths for discrete states in the GTR region of $E_x \approx$ 9–12 MeV. Since these states are situated above the proton separation energy $S_p = 6.31$ MeV, it is suggested that these states are broader due to the decay width. Proton decay widths could be derived for these discrete GT states. The excitation energy dependence of the decay widths could be reasonably well reproduced by the RPA calculations that take the coupling to the continuum (i.e., the proton-decay channel) into account. The peak width of the 13.6 MeV, $T = 2$ GT state situated more than 7 MeV above S_p, however, was not apparently broader than the experimental resolution, suggesting that the proton decay is suppressed. The suppression of the proton decay can be understood in terms of the isospin selection rule that disallows proton decay of $T = 2$ states below $E_x =$ 14.1 MeV.

ACKNOWLEDGMENTS

The (^{3}He,t) experiments were performed at RCNP, Osaka University under the Experimental Program E294. The authors thank the accelerator group of RCNP for providing a high-quality ^{3}He beam. K.W., N.T.K., the Münster group, and the Darmstadt group thank RCNP, Osaka University, Japan for the support during their stay in Osaka. Y.Y.O. acknowledges

the Matsumae International Foundation, Japan for supporting the research stay in Osaka University. G.P.A.B. thanks the support by Japan Society for the Promotion of Science (JSPS), Japan for his stay at RCNP as a guest professor. R.K. acknowledges the support of Graduate School of Science and RCNP during the stay in Osaka University. This work was partly supported by JSPS KAKENHI, Japan under Grants No.15540274, No.18540270, and No. JP15K05104, and by Deutsche Forschungsgemeinschaft (DFG), Germany under contract SFB 1245.

[1] A. Bohr and B. R. Mottelson, *Nuclear Structure* (Benjamin, New York, 1969), Vol. 1.
[2] F. Osterfeld, Rev. Mod. Phys. **64**, 491 (1992), and references therein.
[3] B. Rubio and W. Gelletly, Lect. Notes Phys. **764**, 99 (2009).
[4] J. Rapaport and E. Sugarbaker, Ann. Rev. Nucl. Part. Sci. **44**, 109 (1994).
[5] Y. Fujita, B. Rubio, and W. Gelletly, Prog. in Part. and Nucl. Phys. **66**, 549 (2011), and references therein.
[6] K. Langanke and G. Martínez-Pinedo, Rev. Mod. Phys. **75**, 819 (2003).
[7] T. N. Taddeucci, C. A. Goulding, T. A. Carey, R. C. Byrd, C. D. Goodman, C. Gaarde, J. Larsen, D. Horen, J. Rapaport, and E. Sugarbaker, Nucl. Phys. A **469**, 125 (1987), and references therein.
[8] W. G. Love, K. Nakayama, and M. A. Franey, Phys. Rev. Lett. **59**, 1401 (1987).
[9] R. Madey, B. S. Flanders, B. D. Anderson, A. R. Baldwin, C. Lebo, J. W. Watson, Sam M. Austin, A. Galonsky, B. H. Wildenthal, and C. C. Foster, Phys. Rev. C **35**, 2011 (1987); **36**, 1647 (1987).
[10] Y. Fujita, Y. Shimbara, A. F. Lisetskiy, T. Adachi, G. P. A. Berg, P. von Brentano, H. Fujimura, H. Fujita, K. Hatanaka, J. Kamiya, T. Kawabata, H. Nakada, K. Nakanishi, Y. Shimizu, M. Uchida, and M. Yosoi, Phys. Rev. C **67**, 064312 (2003).
[11] R. G. T. Zegers, H. Akimune, Sam M. Austin, D. Bazin, A. M. van den Berg, G. P. A. Berg, B. A. Brown, J. Brown, A. L. Cole, I. Daito, Y. Fujita, M. Fujiwara, S. Galès, M. N. Harakeh, H. Hashimoto, R. Hayami, G. W. Hitt, M. E. Howard, M. Itoh, J. Jänecke, T. Kawabata, K. Kawase, M. Kinoshita, T. Nakamura, K. Nakanishi, S. Nakayama, S. Okumura, W. A. Richter, D. A. Roberts, B. M. Sherrill, Y. Shimbara, M. Steiner, M. Uchida, H. Ueno, T. Yamagata, and M. Yosoi, Phys. Rev. C **74**, 024309 (2006).
[12] M. N. Harakeh and A. Van Der Woude, *Giant Resonances*, in Oxford Studies in Nucl. Phys. 24 (Oxford University Press, Oxford, 2001).
[13] A. Bohr and B. Mottelson, *Nuclear Structure* (Benjamin, New York, 1975), Vol. 2, Chap. 6, and references therein.
[14] *Isospin in Nuclear Physics*, edited by D. H. Wilkinson (North-Holland, Amsterdam, 1969).
[15] M. S Basunia and A. M. Hurst, Nucl. Data Sheets **134**, 1 (2016).
[16] T. Niizeki, H. Ohnuma, T. Yamamoto, K. Katoh, T. Yamashita, Y. Hara, H. Okamura, H. Sakai, S. Ishida, N. Sakamoto, H. Otsu, T. Wakasa, T. Uesaka, Y. Satou, T. Fujita, T. Ichlhara, H. Orihara, H. Toyokawa, K. Hatanaka, S. Kato, S. Kubono, and M. Yosoi, Nucl. Phys. A **577**, 37c (1994); T. Niizeki (private communication).
[17] See web site http://www.rcnp.osaka-u.ac.jp.
[18] T. Wakasa, K. Hatanaka, Y. Fujita, G. P. A. Berg, H. Fujimura, H. Fujita, M. Itoh, J. Kamiya, T. Kawabata, K. Nagayama, T. Noro, H. Sakaguchi, Y. Shimbara, H. Takeda, K. Tamura, H. Ueno, M. Uchida, M. Uraki, and M. Yosoi, Nucl. Instrum. Methods Phys. Res. A **482**, 79 (2002).
[19] M. Fujiwara, H. Akimune, I. Daito, H. Fujimura, Y. Fujita, K. Hatanaka, H. Ikegami, I. Katayama, K. Nagayama, N. Matsuoka, S. Morinobu, T. Noro, M. Yoshimura, H. Sakaguchi, Y. Sakemi, A. Tamii, and M. Yosoi, Nucl. Instrum. Methods Phys. Res. A **422**, 484 (1999).
[20] T. Noro *et al.*, RCNP (Osaka University), Annual Report, 1991, p. 177.
[21] Y. Fujita, K. Hatanaka, G. P. A. Berg, K. Hosono, N. Matsuoka, S. Morinobu, T. Noro, M. Sato, K. Tamura, and H. Ueno, Nucl. Instrum. Methods Phys. Res. B **126**, 274 (1997), and references therein.
[22] H. Fujita, Y. Fujita, G. P. A. Berg, A. D. Bacher, C. C. Foster, K. Hara, K. Hatanaka, T. Kawabata, T. Noro, H. Sakaguchi, Y. Shimbara, T. Shinada, E. J. Stephenson, H. Ueno, and M. Yosoi, Nucl. Instrum. Methods Phys. Res. A **484**, 17 (2002).
[23] H. Fujita, G. P. A. Berg, Y. Fujita, K. Hatanaka, T. Noro, E. J. Stephenson, C. C. Foster, H. Sakaguchi, M. Itoh, T. Taki, K. Tamura, and H. Ueno, Nucl. Instrum. Methods Phys. Res. A **469**, 55 (2001).
[24] H. Fujita *et al.*, RCNP (Osaka University), Annual Report, 2010, p. 3.
[25] Y. Ichikawa, T. K. Onishi, D. Suzuki, H. Iwasaki, T. Kubo, V. Naik, A. Chakrabarti, N. Aoi, B. A. Brown, N. Fukuda, S. Kubono, T. Motobayashi, T. Nakabayashi, T. Nakamura, T. Nakao, T. Okumura, H. J. Ong, H. Suzuki, M. K. Suzuki, T. Teranishi, K. N. Yamada, H. Yamaguchi, and H. Sakurai, Phys. Rev. C **80**, 044302 (2009).
[26] Y. Fujita, H. Fujita, T. Adachi, G. Susoy, A. Algora, C. L. Bai, G. Colò, M. Csatlós, J. M. Deaven, E. Estevez-Aguado, C. J. Guess, J. Gulyás, K. Hatanaka, K. Hirota, M. Honma, D. Ishikawa, A. Krasznahorkay, H. Matsubara, R. Meharchand, F. Molina, H. Nakada, H. Okamura, H. J. Ong, T. Otsuka, G. Perdikakis, B. Rubio, H. Sagawa, P. Sarriguren, C. Scholl, Y. Shimbara, E. J. Stephenson, T. Suzuki, A. Tamii, J. H. Thies, K. Yoshida, R. G. T. Zegers, and J. Zenihiro, Phys. Rev. C **91**, 064316 (2015).
[27] Y. Shimbara, Y. Fujita, T. Adachi, G. P. A. Berg, H. Fujimura, H. Fujita, K. Fujita, K. Hara, K. Y. Hara, K. Hatanaka, J. Kamiya, K. Katori, T. Kawabata, K. Nakanishi, G. Martìnez-Pinedo, N. Sakamoto, Y. Sakemi, Y. Shimizu, Y. Tameshige, M. Uchida, M. Yoshifuku, and M. Yosoi, Phys. Rev. C **86**, 024312 (2012).
[28] J. C. Hardy and I. S. Towner, Phys. Rev. C **79**, 055502 (2009).
[29] J. C. Hardy and I. S. Towner, Nucl. Phys. News **16**, 11 (2006).
[30] DW81, a DWBA computer code by J. R. Comfort (1981) and updated version (1986), an extended version of DWBA70 by R. Schaeffer and J. Raynal (1970).
[31] S. Y. van der Werf, S. Brandenburg, P. Grasdijk, W. A. Sterrenburg, M. N. Harakeh, M. B. Greenfield, B. A. Brown, and M. Fujiwara, Nucl. Phys. A **496**, 305 (1989).
[32] R. Schaeffer, Nucl. Phys. A **164**, 145 (1971).
[33] R. G. T. Zegers, H. Abend, H. Akimune, A. M. van den Berg, H. Fujimura, H. Fujita, Y. Fujita, M. Fujiwara, S. Galés,

K. Hara, M. N. Harakeh, T. Ishikawa, T. Kawabata, K. Kawase, T. Mibe, K. Nakanishi, S. Nakayama, H. Toyokawa, M. Uchida, T. Yamagata, K. Yamasaki, and M. Yosoi, Phys. Rev. Lett. **90**, 202501 (2003); S. Y. van der Werf and R. G. T. Zegers (private communication).

[34] T. Yamagata, H. Utsunomiya, M. Tanaka, S. Nakayama, N. Koori, A. Tamii, Y. Fujita, K. Katori, M. Inoue, M. Fujiwara, and H. Ogata, Nucl. Phys. A **589**, 425 (1995).

[35] Y. Fujita, T. Adachi, P. von Brentano, G. P. A. Berg, C. Fransen, D. De Frenne, H. Fujita, K. Fujita, K. Hatanaka, E. Jacobs, K. Nakanishi, A. Negret, N. Pietralla, L. Popescu, B. Rubio, Y. Sakemi, Y. Shimbara, Y. Shimizu, Y. Tameshige, A. Tamii, M. Yosoi, and K. O. Zell, Phys. Rev. Lett. **95**, 212501 (2005).

[36] T. Adachi, Y. Fujita, A. D. Bacher, G. P. A. Berg, T. Black, D. De Frenne, C. C. Foster, H. Fujita, K. Fujita, K. Hatanaka, M. Honma, E. Jacobs, J. Jänecke, K. Kanzaki, K. Katori, K. Nakanishi, A. Negret, T. Otsuka, L. Popescu, D. A. Roberts, Y. Sakemi, Y. Shimbara, Y. Shimizu, E. J. Stephenson, Y. Tameshige, A. Tamii, M. Uchida, H. Ueno, T. Yamanaka, M. Yosoi, and K. O. Zell, Phys. Rev. C **85**, 024308 (2012).

[37] H. Fujita, Y. Fujita, T. Adachi, A. D. Bacher, G. P. A. Berg, T. Black, E. Caurier, C. C. Foster, H. Fujimura, K. Hara, K. Harada, K. Hatanaka, J. Jänecke, J. Kamiya, Y. Kanzaki, K. Katori, T. Kawabata, K. Langanke, G. Martínez-Pinedo, T. Noro, D. A. Roberts, H. Sakaguchi, Y. Shimbara, T. Shinada, E. J. Stephenson, H. Ueno, T. Yamanaka, M. Yoshifuku, and M. Yosoi, Phys. Rev. C **75**, 034310 (2007).

[38] Y. Fujita, H. Fujita, T. Adachi, C. L. Bai, A. Algora, G. P. A. Berg, P. von Brentano, G. Colò, M. Csatlós, J. M. Deaven, E. Estevez-Aguado, C. Fransen, D. De Frenne, K. Fujita, E. Ganioğlu, C. J. Guess, J. Gulyás, K. Hatanaka, K. Hirota, M. Honma, D. Ishikawa, E. Jacobs, A. Krasznahorkay, H. Matsubara, K. Matsuyanagi, R. Meharchand, F. Molina, K. Muto, K. Nakanishi, A. Negret, H. Okamura, H. J. Ong, T. Otsuka, N. Pietralla, G. Perdikakis, L. Popescu, B. Rubio, H. Sagawa, P. Sarriguren, C. Scholl, Y. Shimbara, Y. Shimizu, G. Susoy, T. Suzuki, Y. Tameshige, A. Tamii, J. H. Thies, M. Uchida, T. Wakasa, M. Yosoi, R. G. T. Zegers, K. O. Zell, and J. Zenihiro, Phys. Rev. Lett. **112**, 112502 (2014).

[39] E. Ganioğlu, H. Fujita, Y. Fujita, T. Adachi, A. Algora, M. Csatlós, J. M. Deaven, E. Estevez-Aguado, C. J. Guess, J. Gulyás, K. Hatanaka, K. Hirota, M. Honma, D. Ishikawa, A. Krasznahorkay, H. Matsubara, R. Meharchand, F. Molina, H. Okamura, H. J. Ong, T. Otsuka, G. Perdikakis, B. Rubio, C. Scholl, Y. Shimbara, G. Susoy, T. Suzuki, A. Tamii, J. H. Thies, R. G. T. Zegers, and J. Zenihiro, Phys. Rev. C **87**, 014321 (2013).

[40] E. Ganioğlu, H. Fujita, B. Rubio, Y. Fujita, T. Adachi, A. Algora, M. Csatlós, J. M. Deaven, E. Estevez-Aguado, C. J. Guess, J. Gulyás, K. Hatanaka, K. Hirota, M. Honma, D. Ishikawa, A. Krasznahorkay, H. Matsubara, R. Meharchand, F. Molina, H. Okamura, H. J. Ong, T. Otsuka, G. Perdikakis, C. Scholl, Y. Shimbara, G. Susoy, T. Suzuki, A. Tamii, J. H. Thies, R. G. T. Zegers, and J. Zenihiro, Phys. Rev. C **93**, 064326 (2016).

[41] L. Popescu, T. Adachi, G. P. A. Berg, P. von Brentano, D. Frekers, D. De Frenne, K. Fujita, Y. Fujita, E.-W. Grewe, M. N. Harakeh, K. Hatanaka, E. Jacobs, K. Nakanishi, A. Negret, Y. Sakemi, Y. Shimbara, Y. Shimizu, Y. Tameshige, A. Tamii, M. Uchida, H. J. Wörtche, and M. Yosoi, Phys. Rev. C **79**, 064312 (2009).

[42] T. Adachi, Y. Fujita, P. von Brentano, A. F. Lisetskiy, G. P. A. Berg, C. Fransen, D. De Frenne, H. Fujita, K. Fujita, K. Hatanaka, M. Honma, E. Jacobs, J. Kamiya, K. Kawase, T. Mizusaki, K. Nakanishi, A. Negret, T. Otsuka, N. Pietralla, L. Popescu, Y. Sakemi, Y. Shimbara, Y. Shimizu, Y. Tameshige, A. Tamii, M. Uchida, T. Wakasa, M. Yosoi, and K. O. Zell, Phys. Rev. C **73**, 024311 (2006).

[43] Y. Fujita, T. Adachi, H. Fujita, A. Algora, B. Blank, M. Csatlós, J. M. Deaven, E. Estevez-Aguado, E. Ganioğlu, C. J. Guess, J. Gulyás, K. Hatanaka, K. Hirota, M. Honma, D. Ishikawa, A. Krasznahorkay, H. Matsubara, R. Meharchand, F. Molina, H. Okamura, H. J. Ong, T. Otsuka, G. Perdikakis, B. Rubio, C. Scholl, Y. Shimbara, E. J. Stephenson, G. Susoy, T. Suzuki, A. Tamii, J. H. Thies, R. G. T. Zegers, and J. Zenihiro, Phys. Rev. C **88**, 014308 (2013).

[44] C. L. Bai, H. Sagawa, M. Sasano, T. Uesaka, K. Hagino, H. Q. Zhang, X. Z. Zhang, and F. R. Xu, Phys. Lett. B **719**, 116 (2013).

[45] C. L. Bai, H. Sagawa, G. Colò, Y. Fujita, H. Q. Zhang, X. Z. Zhang, and F. R. Xu, Phys. Rev. C **90**, 054335 (2014).

[46] Y. F. Niu, G. Colò, E. Vigezzi, C. L. Bai, and H. Sagawa, Phys. Rev. C **94**, 064328 (2016).

[47] Nguyen Van Giai and H. Sagawa, Phys. Lett. B **106**, 379 (1981).

[48] H. Sagawa, C. L. Bai, and G. Colò, Phys. Scr. **91**, 083011 (2016).

[49] Y. Fujita, Journal of Physics: Conference Series **20**, 107 (2005).

[50] T. Adachi, Y. Fujita, P. von Brentano, G. P. A. Berg, C. Fransen, D. De Frenne, H. Fujita, K. Fujita, K. Hatanaka, M. Honma, E. Jacobs, J. Kamiya, K. Kawase, T. Mizusaki, K. Nakanishi, A. Negret, T. Otsuka, N. Pietralla, L. Popescu, Y. Sakemi, Y. Shimbara, Y. Shimizu, Y. Tameshige, A. Tamii, M. Uchida, T. Wakasa, M. Yosoi, and K. O. Zell, Nucl. Phys. A **788**, 70c (2007).

[51] H. Fujita (private communication).

[52] Y. Fujita, R. Neveling, H. Fujita, T. Adachi, N. T. Botha, K. Hatanaka, T. Kaneda, H. Matsubara, K. Nakanishi, Y. Sakemi, Y. Shimizu, F. D. Smit, A. Tamii, and M. Yosoi, Phys. Rev. C **75**, 057305 (2007).

[53] T. Ichihara, T. Niizeki, H. Okamura, H. Ohnuma, H. Sakai, Y. Fuchi, K. Hatanaka, M. Hosaka, S. Ishida, K. Kato, S. Kato, H. Kawashima, S. Kubono, S. Miyamoto, H. Orihara, N. Sakamoto, S. Takaku, Y. Tajima, M. H. Tanaka, H. Toyokawa, T. Uesaka, T. Yamamoto, T. Yamashita, M. Yosoi, and M. Ishihara, Nucl. Phys. A **569**, 287c (1994).

[54] J. A. Nolen and J. P. Schiffer, Annu. Rev. Nucl. Sci. **19**, 471 (1969).

[55] N. Auerbach, Phys. Rep. **98**, 273 (1983).

[56] Y. Fujita, Y. Shimbara, T. Adachi, G. P. A. Berg, B. A. Brown, H. Fujita, K. Hatanaka, J. Kamiya, K. Nakanishi, Y. Sakemi, S. Sasaki, Y. Shimizu, Y. Tameshige, M. Uchida, T. Wakasa, and M. Yosoi, Phys. Rev. C **70**, 054311 (2004).

[57] G. Colò, N. Van Giai, P. F. Bortignon, and R. A Broglia, Phys. Rev. C **50**, 1496 (1994).

[58] G. F. Bertsch and A. Mekjian, Annu. Rev. Nucl. Sci. **22**, 25 (1972).